Computer Simulations in the Gibbs Ensemble

B. Smit
Shell Research BV
Koninklijke/Shell-Laboratorium Amsterdam
Postbus 3003
1003 AA Amsterdam
The Netherlands

ABSTRACT. The Gibbs ensemble technique is an efficient method to study phase equilibria in a computer simulation. This Chapter gives an overview of this method. The focus is on the principles underlying the method, the practical aspects related to the implementation of the technique, and questions regarding the interpretation of the results.

The practical use of the method is illustrated with applications ranging from polar fluids to chain molecules. In particular, those systems are discussed which require special tricks and extend the range of applicability of the Gibbs method significantly.

1. Introduction

Conceptually, most computer simulations are simple: specify an intermolecular potential and press the 'enter' button. Typically, after a large amount of CPU time the computer reveals everything there is to know about the system. So why worry about techniques to calculate phase equilibria: when the particles phase separate, the interface can be located and the coexistence properties can be 'measured'! Indeed, this would be the case if both the computer and the computer budget were infinite. Unfortunately these limitations make it particularly difficult to study phase equilibria by computer simulations.

To see this, let us consider a system that phase separates into a liquid and a vapour. Assume that the system is equilibrated for sufficiently long so that two interfaces are formed. There are two points to note: firstly, the equilibration requires a very large amount of computer time, often considerably more than for the production run; secondly, since we assume that periodic boundary conditions are used, the formation of two interfaces can be expected. Since the properties of the fluid in the interfacial region differ substantially from the properties in the bulk, we have to discard all the particles in the interfacial region for a 'measurement' of a bulk property.

M.P. Allen and D.J. Tildesley (eds.), Computer Simulation in Chemical Physics, 173–209.

In Table I the percentage of the total number of particles in the interfacial region is given. These numbers show that for a system smaller than 1000 particles the properties are dominated by the interfaces. It is therefore essential to use relatively large systems to calculate reliable coexistence properties. Unfortunately for large systems equilibration requires not only much more CPU time because the systems are big, but also because the equilibration times are longer compared to those of small systems.

A direct calculation of phase equilibria turns out to be 'expensive'. An alternative would be to simulate the vapour and liquid separately and to determine the temperature at which the pressure and chemical potential are equal. Although 'thermal' quantities like the pressure or temperature can be calculated straightforwardly, a simulation does not yield quantities like the free energy or chemical potential directly. The problem of calculating the free energy can be compared with a survey. The percentage of statisticians who believe that statistics are lies, can be determined by a simple poll. The total number of statisticians who believe this, however, requires information on the total number of statisticians. Obtaining this number requires additional work. Similarly in a simulation, the pressure can be calculated from an (extremely) small sample of all possible configurations of the system. The free energy, which is related to the total number of configurations, requires additional techniques. Various methods have been developed to calculate the free energy or chemical potential (see [1] for a review).

TABLE I

The percentage of particles (P_{int}) in the interfacial region. The interfacial region is roughly defined as the volume within 2.5σ from the interface. N is the total number of particles.

N	P_{int}
100	95%
500	55%
1000	44%
10000	20%
50000	10%

One of these methods is to determine the equation-of-state of the system. From the equation-of-state the free energy can be calculated using standard thermodynamic relations [2]. This way of determining the free energy is identical to the experimental method. The method is simple and can be used for almost all systems. However, it requires a large number of equation-of-state points along a reversible path to a state with known free energy (for example the ideal gas limit). With this method the phase diagram of the Lennard-Jones fluid [3, 4] and the two-dimensional Lennard-Jones fluid [5]

have been determined.

A method which yields the excess chemical potential in a single simulation is the Widom particle insertion method [6]. This method utilizes the fact that the change in the free energy in going from N to $N+1$ particles can be expressed as an ensemble average. This ensemble average is calculated by adding test particles to the system. The simulations can now be restricted to the coexistence region since both the pressure and the chemical potential are known. The phase diagram of a quadrupolar Lennard-Jones fluid [7] has been obtained with this method.

The methods described above require either long runs on large systems or many different simulations. Consequently, the calculation of a phase diagram is an elaborate task. A new technique proposed by Panagiotopoulos [8], the so called Gibbs ensemble method, reduces the computer time required for phase equilibrium calculations significantly. With this method, phase equilibria can be studied in a single simulation. The method is particularly useful for studying vapour-liquid and liquid-liquid equilibria. In its present form the method can not be used to study phase equilibria which involve a solid phase.

The Gibbs method utilizes two distinct simulation boxes, which are coupled using Monte Carlo rules. These rules are chosen to ensure that these subsystems are in equilibrium. When a conventional simulation is performed in the two-phase region, droplets of liquid or gas will be formed. In the Gibbs ensemble, the system can lower its free energy by filling one box with vapour and the other with liquid. In this way the formation of interfaces, which increase the free energy because of the interfacial tension between the liquid and the vapour, is avoided. The coexistence properties can be obtained directly from the two boxes. Since this method avoids the interface, it can be used with a relatively small number of particles.

In this Chapter, we study the Gibbs ensemble in detail. The introduction of a new ensemble brings up the question whether it is a 'proper ensemble', i.e. does it yield the same results as the conventional ensembles? To prove it does, we derive in section 2 the partition function and use this function to define a free energy. This free energy is used to show that, in the thermodynamic limit, the Gibbs ensemble and the canonical ensemble are equivalent. This proof gives considerable insight into the 'reason' why the method works.

Having established that the Gibbs ensemble is a sound ensemble, we turn in section 3 to a more practical issue, namely how to sample this ensemble using a Monte Carlo scheme. For this the appropriate acceptance rules are derived. In sections 4 and 5 we describe how the results can be analyzed and the kind of problems one can expect during the simulations. Some applications of the Gibbs ensemble technique are described in section 6. We focus on those applications that involve extensions of the general Gibbs ensemble

method, such as phase equilibria involving dense liquids, mixtures, or chain molecules.

2. Theoretical aspects

In his original article [8], Panagiotopoulos introduced the Gibbs ensemble as a combination of the constant-NVT ensemble, the constant-NPT ensemble, and the constant-μVT ensemble. In this work we take a different point of view, and consider the Gibbs ensemble as a new ensemble [9]. For this ensemble we derive the partition function and define a proper free energy. By considering this free energy we demonstrate that, in the two-phase region, one of the boxes contains the liquid phase and the other the gas phase. Furthermore, we prove that, in the thermodynamic limit, the Gibbs ensemble is equivalent to the canonical ensemble.

2.1. THE PARTITION FUNCTION

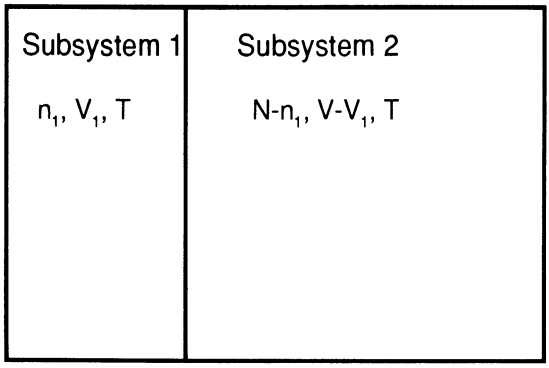

Fig. 1. A schematic picture of the Gibbs ensemble.

Consider a system at constant temperature (T), volume (V), and number of particles (N). This system is divided into two non-interacting subsystems 1 and 2 (see Fig. 1). In a simulation this implies that each box has periodic boundary conditions and particles in one box do *not* interact with the particles in the other box. The particles are distributed over the two subsystems keeping the total number of particles constant. The volume of each subsystem may vary in such a way that the total volume remains constant.

In the partition function of this ensemble, we have to take into account the number of possible distributions of N particles over the two subsystems, to allow for the subsystems to change volume between 0 and V, and to

consider all possible configurations in each subsystem [10–12]

$$\bar{Q}_{NVT} \equiv \frac{1}{V\Lambda^{3N}N!}\sum_{n_1=0}^{N}\binom{N}{n_1}\int_0^V \mathrm{d}V_1 \int_{V_1} \mathrm{d}\mathbf{r}_1^{n_1}\, \exp\left[-\beta\mathcal{V}_1(n_1)\right] \times \int_{V-V_1} \mathrm{d}\mathbf{r}_2^{N-n_1}\, \exp\left[-\beta\mathcal{V}_2(N-n_1)\right], \tag{1}$$

where n_1 denotes the number of particles in box 1, V_1 denotes the volume of box 1, $\mathbf{r}_1^{n_1} = \mathbf{r}_1, \ldots, \mathbf{r}_{n_1}$ and $\mathbf{r}_2^{N-n_1} = \mathbf{r}_{n_1+1}, \ldots, \mathbf{r}_N$ are the positions of the particles in subsystem 1 and subsystem 2 respectively, Λ is the thermal de Broglie wavelength, $\beta = 1/k_B T$, and $\mathcal{V}(n_i)$ is the intermolecular potential.

This partition function will be used in the next section to define the free energy for the Gibbs ensemble, in section 2.3 to derive an expression for the chemical potential, and in section 3 to derive the acceptance rules for Monte Carlo simulations in this ensemble.

2.2. THE FREE ENERGY DENSITY

In this section we study the Gibbs ensemble, as introduced in the previous section in the thermodynamic limit. Before we proceed, we first list a few basic results for the free energy in the canonical ensemble.

2.2.1. Basic definitions and results for the canonical ensemble. Consider a system of N particles in a volume V and temperature T (the canonical ensemble). The partition function is defined as (see Ruelle [13])

$$Q_{NVT} \equiv \frac{1}{\Lambda^{3N}N!}\int_V \mathrm{d}\mathbf{r}^N \exp\left[-\beta\mathcal{V}(N)\right]. \tag{2}$$

The free energy density is defined in the thermodynamic limit by

$$f(\rho) \equiv \lim_{V\to\infty} f_V(\rho) \equiv \lim_{\substack{V\to\infty \\ N/V=\rho}} -\frac{1}{\beta V}\ln Q_{NVT}, \tag{3}$$

where $\rho = N/V$ is the density of the system. For a finite number of particles we can write

$$Q_{NVT} = \exp\left[-\beta V\left(f(\rho) + o(V)\right)\right], \tag{4}$$

where $g(V) = o(V)$ means: $g(V)/V$ approaches zero as $V \to \infty$. With this free energy we can derive some interesting properties of a canonical system in the thermodynamic limit.

For example, it can be shown that this free energy is a convex function of the density ρ [13]

$$f(x\rho_1 + (1-x)\rho_2) \leq xf(\rho_1) + (1-x)f(\rho_2), \tag{5}$$

for every ρ_1, ρ_2, and x where $0 \leq x \leq 1$. The equality holds in the case of a first-order transition, if $\rho_g \leq \rho_1 \leq \rho_2 \leq \rho_l$, where ρ_g, ρ_l denote the density of the coexisting gas and liquid phases respectively (see Figs. 2 (a) and (b)).

(a) no phase transition

(b) a first-order phase transition

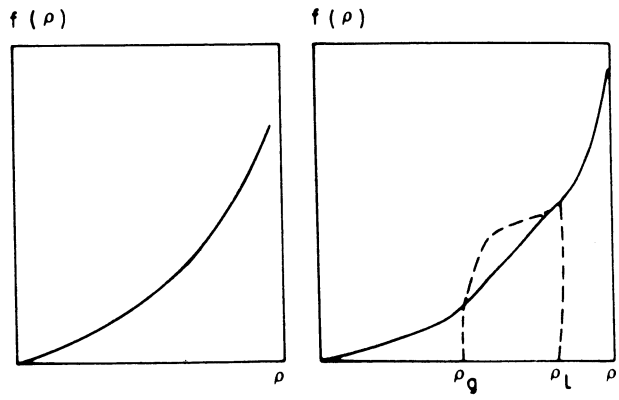

Fig. 2. The free energy density as a function of the density ρ.

Another interesting result, which plays a central rôle in what follows, is the well-known saddle-point theorem [14] (also called the steepest descent method and discussed in Chapter 3). This theorem is based on the observation that, for a macroscopic system (N very large) in equilibrium, the probability that the free energy density deviates from its minimum value is extremely small. Therefore, when we calculate for such a system an ensemble average, we have to take into account only those contributions where the free energy has its minimum value. Assume that Q_{NVT} can be written as

$$Q_{NVT} \equiv \int \mathrm{d}a_1, \ldots, \mathrm{d}a_m \exp\left[-\beta V \left(f_m(a_1, \ldots, a_m) + o(V)\right)\right], \tag{6}$$

where $a_1, \ldots, a_m$ are variables which characterize the thermodynamic state of the system. Furthermore, define

$$f(\rho) \equiv \min_{a_1, \ldots, a_m} f_m(a_1, \ldots, a_m) \tag{7}$$

and assume that $f_m(a_1, \ldots, a_m)$ and the term $o(V)$ satisfy a few technical conditions [14], which hold for most statistical mechanics systems. The saddle-point theorem states that in the thermodynamic limit the free energy

of the system is equal to this minimum value $f(\rho)$ or

$$\lim_{\substack{V\to\infty \\ N/V=\rho}} -\frac{1}{\beta V}\ln Q_{NVT} = f(\rho). \tag{8}$$

Moreover, this saddle-point theorem can also be used to calculate the ensemble average of a quantity $\mathcal{A}$

$$\langle \mathcal{A}(a_1,\ldots,a_m)\rangle_V \equiv \frac{1}{Q_{NVT}}\int \mathrm{d}a_1,\ldots,\mathrm{d}a_m \times \mathcal{A}(a_1,\ldots,a_m)\exp\left[-\beta V\left(f_m(a_1,\ldots,a_m)+o(V)\right)\right]. \tag{9}$$

In the thermodynamic limit, this ensemble average only has contributions from those configurations where $f_m(a_1,\ldots,a_m)$ has its minimum value. Let us define S as the collection of these minima

$$S = \left\{ y_1,\ldots,y_m \,\middle|\, f_m(y_1,\ldots,y_m) = \min_{a_1,\ldots,a_m} f_m(a_1,\ldots,a_m) \right\}. \tag{10}$$

We can now state the saddle-point theorem in a convenient form by introducing a function $G(a_1,\ldots,a_m) \geq 0$ with support on the surface S and normalization

$$\int_S \mathrm{d}a_1,\ldots,\mathrm{d}a_m\, G(a_1,\ldots,a_m) = 1 \tag{11}$$

such that, for an arbitrary function $\mathcal{A}$

$$\langle \mathcal{A}(a_1,\ldots,a_m)\rangle \equiv \lim_{V\to\infty}\langle \mathcal{A}(a_1,\ldots,a_m)\rangle_V = \int_S \mathrm{d}a_1,\ldots,\mathrm{d}a_m\, G(a_1,\ldots,a_m)\mathcal{A}(a_1,\ldots,a_m). \tag{12}$$

2.2.2. The free energy density in the Gibbs ensemble. The Gibbs ensemble is introduced in section 2.1 as a constant-NVT ensemble to which an additional degree of freedom is added: the system is divided into two subsystems which have *no* interactions with each other. We can rewrite the partition function of the canonical ensemble as (eqn (2))

$$Q_{NVT} = \frac{1}{\Lambda^{3N}N!}\sum_{n_1=0}^{N}\binom{N}{n_1}\int_0^V \mathrm{d}V_1 \int \mathrm{d}\mathbf{r}_1^{n_1}\int \mathrm{d}\mathbf{r}_2^{N-n_1} \times \exp\left[-\beta\left(\mathcal{V}_1(n_1) + \mathcal{V}_2(N-n_1) + \text{interactions between the two volumes}\right)\right]. \tag{13}$$

The difference between this equation and the partition function of the Gibbs ensemble, eqn (1), is that in eqn (2) we do have interactions between the subsystems. In the case of short-range interactions, the last term in the exponent of eqn (13) is proportional to a surface term. This already suggests

that both ensembles should behave similarly in many respects. We expound these ideas more rigorously in the following pages.

In the usual way, we define the free energy in the Gibbs ensemble as

$$\bar{f}(\rho) \equiv \lim_{\substack{V\to\infty \\ N/V=\rho}} -\frac{1}{\beta V} \ln \bar{Q}_{NVT}. \tag{14}$$

In the partition function of the Gibbs ensemble, eqn (1), we can substitute eqn (2)

$$\bar{Q}_{NVT} = \sum_{n_1=0}^{N} \int_0^V \mathrm{d}V_1 \; Q_{n_1,V_1,T} Q_{N-n_1,V-V_1,T}. \tag{15}$$

Introducing $x = N_1/N$ and $y = V_1/V$, and assuming that the number of particles is very large, we can write

$$\bar{Q}_{NVT} = NV \int_0^1 \mathrm{d}x \int_0^1 \mathrm{d}y \, \bar{Q}_N(x,y), \tag{16}$$

where

$$\begin{aligned} \bar{Q}_N(x,y) &= Q_{xN,yV,T} \, Q_{(1-x)N,(1-y)V,T} \\ &= \exp\left[-\beta V \left\{ y f\left(\frac{x}{y}\rho\right) + (1-y) f\left(\frac{1-x}{1-y}\rho\right) + o(V) \right\}\right]. \end{aligned} \tag{17}$$

Note that in this equation $f(\rho)$ is the free energy of a canonical system. So, we can apply the saddle-point theorem of the previous section (eqn (8)) to calculate the free energy density of the Gibbs ensemble $\bar{f}(\rho)$

$$\bar{f}(\rho) = \min_{\substack{0<x<1 \\ 0\le y\le 1}} \left\{ y f\left(\frac{x}{y}\rho\right) + (1-y) f\left(\frac{1-x}{1-y}\rho\right) \right\} \equiv \min_{\substack{0<x<1 \\ 0\le y\le 1}} \left\{ \bar{f}(x,y) \right\}. \tag{18}$$

We now have to find the surface S on which the function $\bar{f}(x,y)$ reaches its minimum. For this we can use the fact that $f(\rho)$ is a convex function of the density (eqn (5)). This gives for $\bar{f}(x,y)$

$$\bar{f}(x,y) \ge f\left(y\frac{x}{y}\rho + (1-y)\frac{1-x}{1-y}\rho \right) = f(\rho). \tag{19}$$

We first consider the case where there is only one phase. For this case the free energy $f(\rho)$ is shown schematically as a function of the density in Fig. 2 (a). This figure demonstrates that any combination of x and y, which result in densities ρ_1 and ρ_2 in the subsystems different from ρ, will give a higher free energy. So, the equality in eqn (19) holds only if

$$\frac{x}{y}\rho = \frac{1-x}{1-y}\rho, \quad \text{or} \quad x = y. \tag{20}$$

Thus, in the case where there is only one phase, the free energy of the Gibbs ensemble has its minimum value (in the thermodynamic limit) when both boxes have a density equal to the equilibrium density of the canonical ensemble. Therefore, the surface S is given by

$$S = \{(x, y) \,|x = y\}\,. \tag{21}$$

Secondly, we consider the case of a first-order phase transition, for which the free energy as a function of the density is shown in Fig. 2 (b). Let ρ be such that $\rho_l \leq \rho \leq \rho_g$, and let us choose x and y such that

$$\rho_g \leq \frac{x}{y}\rho \equiv \rho_3 \leq \rho_l \quad \text{and} \quad \rho_g \leq \frac{1-x}{1-y}\rho \equiv \rho_4 \leq \rho_l. \tag{22}$$

For this case the equality in eqn (5) holds and we can write for $\bar{f}(x, y)$

$$\begin{aligned} \bar{f}(x, y) &= yf(\rho_3) + (1-y)f(\rho_4), \\ &= f(y\rho_3 + (1-y)\rho_4). \end{aligned} \tag{23}$$

Note that

$$(y\rho_3 + (1-y)\rho_4) = \rho, \tag{24}$$

which gives

$$\bar{f}(x, y) = f(\rho). \tag{25}$$

It can be shown that, if x, y do not satisfy eqn (22),

$$\bar{f}(x, y) > f(\rho). \tag{26}$$

Therefore, the surface S in the case of a first-order phase transition is given by

$$S = \left\{(x, y) \,\middle|\, \rho_g \leq \frac{x}{y}\rho \leq \rho_l, \quad \rho_g \leq \frac{1-x}{1-y}\rho \leq \rho_l \right\}. \tag{27}$$

This result shows that, in the case of a first-order transition, the (bulk) free energy of the Gibbs ensemble has its minimum value (in the thermodynamic limit) for all values of x, y where there is vapour-liquid coexistence in *both* boxes.

Equations (19) and (25) show that in the thermodynamic limit the free energy of the Gibbs ensemble is equal to the free energy of the canonical ensemble. In order to calculate an ensemble average, it simply remains to determine the function $G(x, y)$ (cf. eqn (12)).

In the case of a pure phase $G(x, y)$ needs to be of the form

$$G(x, y) = g(x)\,\delta(x - y). \tag{28}$$

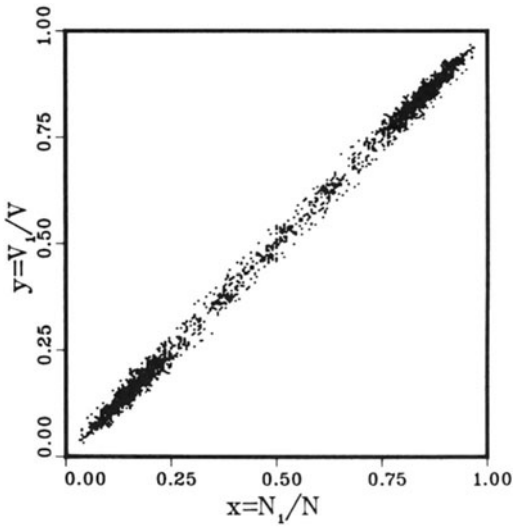

Fig. 3. A probability plot in the x, y plane ($x = n_l/N, y = V_l/V$) for a Lennard-Jones fluid at high temperature ($T = 5.21$, $N = 216$ and $V = 670$). The total number of cycles in this simulation was 6000 (see section 3 for details on the simulations). After every 6 cycles the points (x_i, y_i) and $(1 - x_i, 1 - y_i)$ were plotted in the x, y plane.

As shown the appendix of Ref. [9], $g(x) = 1$ for the ideal gas. We expect the same to be true for an interacting gas. Fig. 3 shows a probability plot in the x, y plane for a simulation of a finite system at high temperature. This figure shows that $x \approx y$. We have not attempted to estimate $g(x)$.

In the case of two phases we will show that the system will split into a liquid phase, with density ρ_l, in one box, and a vapour phase, with density ρ_g, in the other box.

Until now we have ignored surface effects, which arise from the presence of a liquid-vapour interface in the boxes. When the density in one of the boxes is between the vapour and liquid density, the system will form droplets of gas or liquid. The interfacial free energy associated with these droplets has (in the thermodynamic limit) a negligible contribution to the bulk free energy of the Gibbs ensemble. Nevertheless, it turns out that this surface free energy is the driving force that causes the system to separate into a homogeneous liquid in one box and a homogeneous vapour phase in the other.

These surface effects are taken into account in the next significant term in the expression for the free energy (eqn (4)), which is the term due to the

surface tension. This gives, for the partition function,

$$Q_{NVT} = \exp\left[-\beta\left(Vf(\rho) + \gamma A + o(A)\right)\right], \tag{29}$$

where A denotes the area of the interface and γ denotes the interfacial tension. For three-dimensional systems this area will in general be proportional to $V^{2/3}$. using this form of the partition function for the Gibbs ensemble, eqn (9) can be written as

$$\langle \mathcal{A}(x,y)\rangle_V = \frac{\iint \mathrm{d}x\mathrm{d}y\, \mathcal{A}(x,y) \exp\left[-\beta\left(Vf(x,y) + \gamma V^{2/3} a(x,y) + o(V^{2/3})\right)\right]}{Q_{NVT}}, \tag{30}$$

where $a(x,y)$ is a function of the order of unity.

We know from the saddle-point theorem that the most important contribution to the integrals comes from the region S, defined by eqn (27). Thus

$$\begin{aligned}\langle \mathcal{A}(x,y)\rangle_V &\approx \frac{\iint_S \mathrm{d}x\mathrm{d}y\, \mathcal{A}(x,y) \exp\left[-\beta\left(Vf(x,y) + \gamma V^{2/3} a(x,y) + o(V^{2/3})\right)\right]}{\iint_S \mathrm{d}x\mathrm{d}y \exp\left[-\beta\left(Vf(x,y) + \gamma V^{2/3} a(x,y) + o(V^{2/3})\right)\right]} \\ &= \frac{\iint_S \mathrm{d}x\mathrm{d}y\, \mathcal{A}(x,y) \exp\left[-\beta\left(\gamma V^{2/3} a(x,y) + o(V^{2/3})\right)\right]}{\iint_S \mathrm{d}x\mathrm{d}y \exp\left[-\beta\left(\gamma V^{2/3} a(x,y) + o(V^{2/3})\right)\right]}\end{aligned} \tag{31}$$

and, applying the saddle-point theorem again,

$$\langle \mathcal{A}(x,y)\rangle_V \approx \frac{\iint_{S_A} \mathrm{d}x\mathrm{d}y\, \mathcal{A}(x,y) \exp\left[-\beta\gamma V^{2/3} a(x,y) + o(V^{2/3})\right]}{\iint_{S_A} \mathrm{d}x\mathrm{d}y \exp\left[-\beta\gamma V^{2/3} a(x,y) + o(V^{2/3})\right]} \tag{32}$$

and

$$\lim_{V\to\infty} \langle \mathcal{A}(x,y)\rangle_V = \iint_{S_A} \mathrm{d}x\mathrm{d}y\, G(x,y)\, \mathcal{A}(x,y), \tag{33}$$

where the surface S_A is now given by

$$S_A = \left\{(x,y) \,\middle|\, a(x,y) = \min_{\bar{x},\bar{y}} a(\bar{x},\bar{y})\right\}. \tag{34}$$

In the infinite system it is easily seen that the area of the interface is zero, if box 1 contains only gas (liquid) and box 2 only liquid (gas). Therefore, the surface S_A contains only two points, which corresponds to the vapour and liquid density

$$S_A = \left\{(x,y) \,\middle|\, \frac{x}{y} = \rho_{\mathrm{l}} \text{ and } \frac{1-x}{1-y} = \rho_{\mathrm{g}} \text{ or } \frac{x}{y} = \rho_{\mathrm{g}} \text{ and } \frac{1-x}{1-y} = \rho_{\mathrm{l}}\right\}. \tag{35}$$

It is straightforward to show that this surface gives for $G(x,y)$

$$G(x,y) = \frac{1}{2}\delta\left(x - \frac{\rho_g}{\rho}\frac{\rho-\rho_g}{\rho_l-\rho_g}\right)\delta\left(y - \frac{\rho-\rho_g}{\rho_l-\rho_g}\right) + \frac{1}{2}\delta\left(x - \frac{\rho_l}{\rho}\frac{\rho_l-\rho}{\rho_l-\rho_g}\right)\delta\left(y - \frac{\rho_l-\rho}{\rho_l-\rho_g}\right). \tag{36}$$

2.2.3. Summary. In this section, we have shown more formally that the free energy density for the Gibbs ensemble, as defined by eqn (14), becomes identical to the free energy density of the canonical ensemble.

Furthermore, it is shown that, at high temperatures, $x = y$, i.e. the densities in the two subsystems of the Gibbs ensemble are equal, and equal to the density in the canonical ensemble (see Fig. 3).

In the case of a first-order phase transition, if surface terms are unimportant, then x and y are restricted to the area defined by (cf. eqn (27))

$$\rho_g \leq \frac{x}{y}\rho \equiv \rho_3 \leq \rho_l \quad \text{and} \quad \rho_g \leq \frac{1-x}{1-y}\rho \equiv \rho_4 \leq \rho_l. \tag{37}$$

If we take surface effects into account, it is shown that this surface (eqn (37)) reduces to two points in the x,y plane. The densities of these points correspond to the density of the gas or liquid phase in the canonical ensemble.

It is interesting to compare this with the results of an actual simulation of a finite system. In Fig. 4 the results for a simulation at a temperature well below the critical point are given. This shows that the surface reduces to two points. This should be compared to the results of a simulation close to the critical point (Fig. 5). At those conditions the interfacial tension is very small and we see that the simulation samples the entire surface S. Note that, due to the finite size of this system, fluctuations are also possible in which the density of a subsystem becomes greater/smaller than the density of the liquid/gas phase.

2.3. THE CHEMICAL POTENTIAL

One of the steps in the Gibbs ensemble involves the insertion of a particle in one of the boxes. During this step, the energy of this particle has to be calculated (see section 3). Since this energy corresponds to the energy of a test particle, we can use the Widom insertion method [6] to calculate the chemical potential without additional costs [15]. At this point, it is important to note that the Gibbs method does not require computation of the chemical potentials. However, in order to test whether the system under consideration has reached equilibrium, or for comparison with other results, it is important to calculate the chemical potential of the individual phases correctly. The

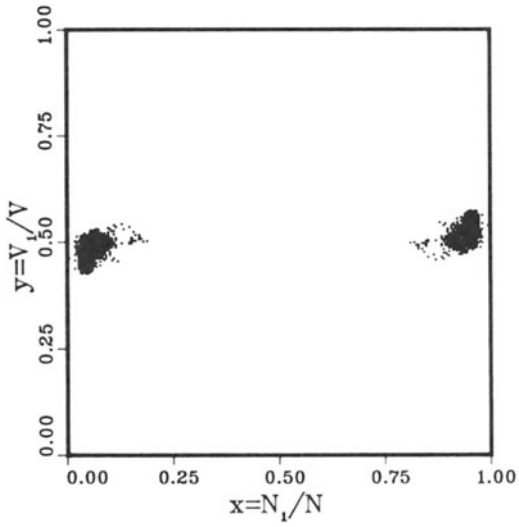

Fig. 4. A probability plot in the x, y plane for a Lennard-Jones fluid well below the critical temperature ($T = 1.15, N = 216, V = 670$); see also the caption to figure 3.

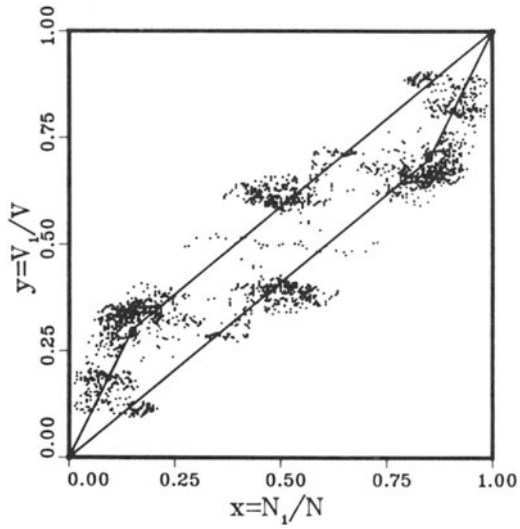

Fig. 5. A probability plot in the x, y plane for a Lennard-Jones fluid slightly below the critical temperature ($T = 1.30, N = 512, V = 1600$). The solid lines show the area S as defined in eqn (27); see also the caption to Fig. 3.

original Widom expression is only valid in the canonical ensemble. It can be modified for applications in the isothermal-isobaric ensemble [16, 17] or the microcanonical ensemble [1]. Here we derive an expression for the chemical potential for the Gibbs ensemble. We restrict ourselves to temperatures sufficiently far below the critical temperature such that the two boxes, after equilibration, do not change identity. For the more general case we refer to Ref. [11].

If we rescale the coordinates of the particles with the box length, the partition function for the Gibbs ensemble, eqn (1), becomes

$$\begin{aligned}\bar{Q}_{NVT} \equiv & \frac{1}{V\Lambda^{3N}N!}\sum_{n_1=0}^{N}\binom{N}{n_1}\int_0^V \mathrm{d}V_1\, V_1^{n_1}(V-V_1)^{N-n_1} \\ & \times \int \mathrm{d}\boldsymbol{\xi}_1^{n_1}\, \exp\left[-\beta\mathcal{V}_1(n_1)\right]\int \mathrm{d}\boldsymbol{\xi}_2^{N-n_1}\, \exp\left[-\beta\mathcal{V}_2(N-n_1)\right], \\ = & \sum_{n_1=0}^{N}\int_0^V \mathrm{d}V_1\, V_1^{n_1}(V-V_1)^{N-n_1} Q_1(n_1,V_1)\, Q_2(N-n_1,V-V_1),\end{aligned} \tag{38}$$

where $\boldsymbol{\xi} = \mathbf{r}/L$ is the scaled coordinate vector of a particle, L is the box length of the subsystem in which the particle is located, and $Q_i(n_i, V_i)$ is the partition function of the canonical ensemble (see also section 2.2.2).

The chemical potential of box 1 can be defined as

$$\begin{aligned}\mu_1 \equiv & -k_\mathrm{B}T\ln\sum_{n_1=0}^{N}\int_0^V \mathrm{d}V_1\, V_1^{n_1}(V-V_1)^{N-n_1} \\ & \times\left(\frac{Q_1(n_1+1,V_1)}{Q_1(n_1,V_1)}\right) Q_2(N-n_1,V-V_1).\end{aligned} \tag{39}$$

For the ratio of the partition functions of box 1 we can write

$$\begin{aligned}\frac{Q_1(n_1+1,V_1)}{Q_1(n_1,V_1)} &= \frac{V_1}{(n_1+1)\Lambda^3}\frac{\int \mathrm{d}\boldsymbol{\xi}_1^{n_1+1}\, \exp\left[-\beta\mathcal{V}_1(n_1+1)\right]}{\int \mathrm{d}\boldsymbol{\xi}_1^{n_1}\, \exp\left[-\beta\mathcal{V}_1(n_1)\right]} \\ &= \frac{V_1}{(n_1+1)\Lambda^3}\frac{\int \mathrm{d}\boldsymbol{\xi}_1^{n_1}\, \exp\left[-\beta\Delta v_1^+\right]\exp\left[-\beta\mathcal{V}_1(n_1)\right]}{\int \mathrm{d}\boldsymbol{\xi}_1^{n_1}\, \exp\left[-\beta\mathcal{V}_1(n_1)\right]},\end{aligned} \tag{40}$$

in which we have used the notation

$$\mathcal{V}_1(n_1+1) = \Delta v_1^+ + \mathcal{V}_1(n_1), \tag{41}$$

where Δv_1^+ is the test particle energy of a (ghost) particle in box 1. We can write eqn (39) as an ensemble average restricted to box 1

$$\mu_1 = -k_\mathrm{B}T\ln\frac{1}{\Lambda^3}\left\langle\frac{V_1}{n_1+1}\exp\left[-\beta\Delta v_1^+\right]\right\rangle_{\text{Gibbs, box 1}}, \tag{42}$$

where $\langle \ldots \rangle_{\text{Gibbs, box } i}$ denotes an ensemble average in the Gibbs ensemble restricted to box i (note that this ensemble average is well defined if the boxes do not change identity during a simulation).

3. Computational aspects

In section 2.1, the partition function of the Gibbs ensemble was derived and it was shown that in the two-phase region one of the sub-systems contains the vapour phase and the other subsystem the liquid phase. This property makes the Gibbs ensemble a convenient ensemble to study vapour-liquid (or liquid-liquid) phase equilibria. In this section we describe a Monte Carlo procedure which samples the Gibbs ensemble.

3.1. ACCEPTANCE RULES

The problem of devising a procedure which generates configurations with a specific probability distribution, can be formulated conveniently in terms of the theory of stochastic processes (van Kampen [18]). For example, one can generate a chain of configurations by specifying a Markov process, in which a new configuration $\mathbf{\Gamma}_m$ is obtained from the old configuration $\mathbf{\Gamma}_n$ with a transition probability $T_{(m|n)}$

$$\mathbf{\Gamma}_m = T_{(m|n)} \mathbf{\Gamma}_n \,. \tag{43}$$

Repetition of this procedure generates a chain of configurations (Markov chain). The conditions which need to be fulfilled by this transition probability to obtain configurations with the desired probability distribution are outlined by Feller [19, 20] or van Kampen [18]:

- the Markov chain needs to be *ergodic*, i.e. all possible configurations must be within reach from any other configuration in a finite number of steps;
- the transition probability must satisfy the condition of *detailed balance*, i.e. the number of transitions from configuration m to n must be equal to the number of transitions from n to m

  $$K_{(n|m)} = K_{(m|n)} \,. \tag{44}$$

  The number of transitions $K_{(n|m)}$ is the product of the statistical weight of configuration n (N_n) and the acceptance probability

  $$K_{(n|m)} = N_n \, \mathrm{acc}(n|m) \,. \tag{45}$$

The condition of detailed balance is stronger than strictly necessary to obtain an equilibrium distribution [18]. However, it has an important practical advantage. The condition of detailed balance guarantees that the equilibrium distribution will be reached in the course of a Markov process *irrespective* of the form of this distribution. Therefore, by imposing detailed balance we

are guaranteed that the Markov chain will give the correct distribution of configurations for the Gibbs ensemble.

From the partition function of the Gibbs ensemble, it follows that we have to displace the particles in the two boxes, change the volume of the subsystems, and exchange particles between the boxes. Here we consider the version of the Gibbs ensemble where the total number of particles and the total volume of the two boxes remains constant, i.e. the total system is at constant-NVT conditions. The appropriate acceptance rules for the constant-NPT version can be found in Ref. [15].

In the Gibbs ensemble, the statistical weight of a configuration m with n_1 particles in box 1 with volume V_1, and $N - n_1$ particles in box 2 with volume $V - V_1$ is proportional to (cf. eqn (1))

$$N_m \propto \frac{V_1^{n_1}(V - V_1)^{N-n_1}}{n_1!(N - n_1)!} \exp(-\beta \mathcal{V}_m) , \tag{46}$$

where $\mathcal{V}_m$ is the total potential energy (sum of the energy of box 1 and box 2).

The acceptance rules can be derived from fluctuation theory [8, 15] or directly from the partition function [10, 11]. Here we derive the acceptance rules using the condition of detailed balance.

For example, assume that state n is obtained from state m via the displacement of a particle in box 1. The ratio of the statistical weights of these two configurations is given by

$$\frac{N_n}{N_m} = \exp[-\beta(\mathcal{V}_n - \mathcal{V}_m)] . \tag{47}$$

Substituting eqn (47) into eqn (45), we find that the following acceptance rule for a particle displacement will satisfy the detailed balance condition, eqn (44)

$$\mathrm{acc}(m|n) = \min\{1, \exp[-\beta(\mathcal{V}_n - \mathcal{V}_m)]\} . \tag{48}$$

For a change of the volume of box 1 by an amount ΔV, the ratio of the statistical weights of the configurations after and before the move is given by

$$\frac{N_n}{N_m} = \frac{(V_1 + \Delta V)^{n_1}(V - (V_1 + \Delta V))^{N-n_1}}{V_1^{n_1}(V - V_1)^{N-n_1}} \exp[-\beta(\mathcal{V}_n - \mathcal{V}_m)] . \tag{49}$$

Imposing the condition of detailed balance gives as acceptance rule for the volume change

$$\mathrm{acc}(m|n) = \min\left\{1, \frac{(V_1 + \Delta V)^{n_1}(V - (V_1 + \Delta V))^{N-n_1}}{V_1^{n_1}(V - V_1)^{N-n_1}} \exp[-\beta(\mathcal{V}_n - \mathcal{V}_m)]\right\} . \tag{50}$$

If the configuration n is obtained from configuration m by removing a particle from box 1 and inserting this particle in box 2, the ratio of statistical weights is given by

$$\frac{N_n}{N_m} = \frac{n_1!(N-n_1)!V_1^{n_1-1}(V-V_1)^{N-(n_1-1)}}{(n_1-1)!(N-(n_1-1))!V_1^{n_1}(V-V_1)^{N-n_1}} \exp[-\beta(\mathcal{V}_n-\mathcal{V}_m)] \,. \quad (51)$$

Again, imposing detailed balance for a particle exchange move leads to the acceptance rule

$$\mathrm{acc}(m|n) = \min\left\{1, \frac{n_1(V-V_1)}{(N-n_1+1)V_1} \exp[-\beta(\mathcal{V}_n - \mathcal{V}_m)]\right\} . \quad (52)$$

The moves described above are identical to the ones proposed by Panagiotopoulos *et al.* in Refs. [8, 15]. A more natural choice for generating a new configuration in the volume-change step, is to make a random walk in $\ln(V_1/(V-V_1))$ instead of in V_1 (see also Ref. [21] for the NPT ensemble). This has the advantage that the domain of this random walk coincides with the possible values of V_1. Furthermore, the average step size turns out to be less sensitive to the density. In order to adopt this method for the Gibbs ensemble, the acceptance rule for the volume has to be modified. If we make a random walk in $\ln(V_1/(V-V_1))$, the ensemble averages that are calculated correspond to

$$\begin{aligned}\langle \mathcal{A} \rangle \;=\; & \frac{1}{Q_{NVT}} \frac{1}{\Lambda^{3N} N!} \sum_{n_1=0}^{N} \\ & \times \binom{N}{n_1} \int_{-\infty}^{\infty} \mathrm{d}\ln\left(\frac{V_1}{V-V_1}\right) \frac{V_1(V-V_1)}{V} V_1^{n_1}(V-V_1)^{N-n_1} \\ & \times \int \mathrm{d}\xi_1^{n_1} \exp\left[-\beta\mathcal{V}_1(n_1)\right] \int \mathrm{d}\xi_2^{N-n_1} \exp\left[-\beta\mathcal{V}_2(N-n_1)\right] \mathcal{A}(\xi^N) \end{aligned} \quad (53)$$

The statistical weight of a configuration m is now proportional to

$$N_m \propto \frac{V_1^{n_1+1}(V-V_1)^{N-n_1+1}}{V n_1!(N-n_1)!} \exp(-\beta\mathcal{V}_m) \,. \quad (54)$$

Imposing detailed balance for this move leads to the acceptance rule

$$\begin{aligned}&\mathrm{acc}(m|n) = \\ &\quad \min\left\{1, \left(\frac{V_1^n}{V_1^m}\right)^{n_1+1} \left(\frac{V-V_1^n}{V-V_1^m}\right)^{N-n_1+1} \exp[-\beta(\mathcal{V}_n - \mathcal{V}_m)]\right\} , \end{aligned} \quad (55)$$

in which V_1^m denotes the volume of box 1 of configuration m. The acceptance rules for the particle displacement or particle exchange are not affected.

3.2. COMPUTATIONAL ASPECTS

A convenient method to generate trial configurations is to perform a simulation in cycles. One cycle consists of (on average) N_{disp} attempts to displace a (random) particle in one of the (randomly chosen) boxes, N_{vol} attempts to change the volume of the subsystems, and N_{try} attempts to exchange particles between the boxes. It is important to ensure that at each step of the simulation the condition of microscopic reversibility is fulfilled (see for example the algorithm described in Fig. 6).

```
Npart1 : number of particles in box 1
Npart2 : number of particles in box 2
Nvol   : number of attempts to change the volume
Ntry   : number of attempts to exchange particles
Ncycle : number of Monte Carlo cycles


nvar = Npart1+Npart2+Nvol+Ntry
DO icl = 1,Ncycle
   DO ivar = 1,nvar
      ran = random_number
      IF (ran .LE. Npart1/nvar) THEN
         displace_particle_in_box_1
      ELSE IF (ran .LE. (Npart1+Npart2)/nvar) THEN
         displace_particle_in_box_2
      ELSE IF (ran .LE. (Npart1+Npart2+Nvol)/nvar) THEN
         change_volume
      ELSE IF (ran .LE. (Npart1+Npart2+Nvol+0.5*Ntry)/nvar) THEN
         exchange_particle_from_box_1_to_box_2
      ELSE
         exchange_particle_from_box_2_to_box_1
      ENDIF
   ENDDO
ENDDO
```

Fig. 6. The basic algorithm for a computer simulation in the Gibbs ensemble.

In most applications of the Gibbs ensemble, the simulations were performed slightly differently; instead of making a random choice at each Monte Carlo step which type of change (particle displacement, volume change, or particle exchange) will be made, the simulations were performed in a strict order. First, an attempt to displace each particle successively (the 'NVT

part'), then an attempt to change the volume (the 'NPT part'), and finally N_{try} attempts to exchange particles (the 'μVT part'). Although, with this scheme, microscopic reversibility is not fulfilled at every step in the algorithm, it can be expected that this method of generating new configurations will also lead to the correct probability distributions. However, the scheme described in the previous paragraph has some practical advantages. For example, there is no ambiguity when to sample a configuration, one does not have to make the choice of sampling after the NVT part, the NPT part, or the μVT part, but one can simply sample after each n^{th} cycle.

A more serious disadvantage of the successive method is that in the latter scheme, when the probability of acceptance of an exchange becomes greater than 3%, erroneous can results occur. In Ref. [8] a bias in the liquid pressure was observed, which disappeared when the number of attempts to exchange particles was reduced. In section 4 it is shown that one should be extremely careful with this, since a simulation in the Gibbs ensemble can become easily trapped in such a region.

The details of the implementation of each step of the simulation depend on the intermolecular potential and on the conditions of the system. A general rule which should be considered in the implementation is that the simulation samples the configuration space efficiently. What efficient sampling means can be illustrated with a quotation from Ref. [10]:

> ...In very vague terms, sampling is efficient if it gives you good value for money. 'Good value' in a simulation corresponds to high statistical accuracy and 'money' is simply *money:* the money that buys your computer or even your own time. Let us assume that you are very poorly paid. In that case we only have to worry about your computer budget. Then we could use the following definition of an optimum sampling scheme: *A Monte Carlo sampling scheme can be considered optimum, if it yields the lowest statistical error in the quantity to be computed for a given expenditure of 'computer budget'.* ...it is reasonable to assume that the mean-square error is inverse proportional to the number of 'uncorrelated' configurations visited in a given amount of CPU time. ...

Below, some general points are made concerning the efficiency of the various steps in the Gibbs ensemble. However, one should be careful in applying these general rules for a particular system. Various examples exist where the optimal algorithm deviates significantly from these general rules. In section 6 some examples of these exceptions are described.

A particle displacement. In this step, a particle in one of the boxes is chosen at random and given a random displacement. The maximum displacement must be chosen in such a way that the sampling is efficient. For example, in the case of the Lennard-Jones potential the amount of CPU required to calculate the energy difference for a given trial move is independent

of whether this move is rejected or accepted. Therefore, in this case the maximum displacement is set to give an acceptance ratio of approximately 50%. For other potentials, the optimum acceptance ratio can deviate significantly from this 50% (see section 6).

A volume change. In this step the volume of the boxes is changed in such a way that the total volume remains constant (in the case where the constant-NPT version of the Gibbs ensemble is used, the volumes of the two boxes are changed independently). For some systems, we can use the scaling properties of the intermolecular potential to calculate the energy of the new configuration efficiently (see Refs. [22, 23]).

Again, the maximum change of the volume must be chosen using the criterion of efficiency. In the case of the Lennard-Jones potential, there is no difference in required CPU time between an accepted and a rejected move. Therefore for this potential an acceptance ratio of approximately 50% is appropriate.

A particle exchange. In this step, a particle is exchanged between the two subsystems. Inspection of the main algorithm shows that a box, from which a random particle is to be deleted, is chosen at random. This particle will be placed at a random position in the other box.

The number of attempts to exchange a particle will depend on the conditions of the system. For example, it can be expected that close to the critical temperature the percentage of accepted exchanges will be higher than close to the triple point. A possible check whether the number of attempts is sufficient, is to calculate the chemical potential. Since the calculated energy of a particle which is to be inserted corresponds to just the test-particle energy, the chemical potential can be calculated without additional costs.

In Ref. [8] it is mentioned that close to the critical point some simulations failed because one of the boxes became empty. However, inspection of the partition function (eqn (1)) shows that one must allow for $n_1 = 0$ (box one empty) and $n_1 = N$ (box two empty) in order to calculate ensemble averages correctly. So, it is important to ensure that the program does not fail because of technical reasons when one of the boxes becomes empty. For example, when one of the boxes is empty the addition of yet another particle to the full box may cause a division by zero. This addition will lead to a situation with $N+1$ particles and inspection of the partition function shows that this configuration should not be sampled. However, if one also calculates the chemical potential during the exchange step one should be careful. In order to calculate the chemical potential correctly (see section 2.3) one should also add *test particles* when one of the boxes is full.

4. Finite-size effects

Computer simulations are usually performed on a relatively small number of particles. The results of these simulations will in general depend on the system size. Because we are usually interested in the infinite system, it is important to estimate the magnitude of the finite-size effects. For example, it is well known that the critical temperature of a finite system decreases when the system size is increased. For a finite system a true critical point does not exist. However, one can observe a pseudo-critical temperature when the fluctuations in the density are correlated over distances of the order of the system size. For lattice models, these finite-size effects have been studied in great detail using finite-size scaling techniques [24]. Here we analyze the finite-size effects that are specific to the Gibbs ensemble using the theoretical framework developed in section 2.

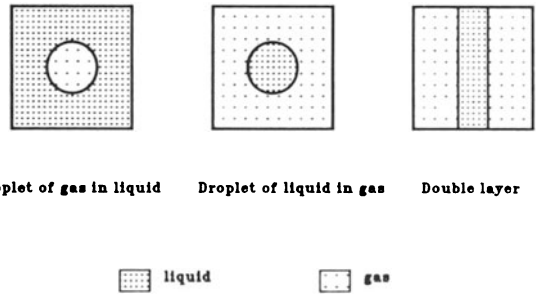

Fig. 7. A schematic representation of one of the boxes in a Monte Carlo simulation in the Gibbs ensemble slightly below the critical temperature.

For the infinite system we have shown that, in the case of a first-order phase transition, one of the subsystems will contain the gas (liquid) phase and the other subsystem will contain the liquid (gas) phase. For small systems we can expect to observe configurations that differ from the pure liquid or gas densities. The penalty of these deviations is related to the free energy increase caused by the formation of droplets of the other phase. Since the chemical potentials of the two phases are equal, this free energy increase arises from the surface between the two phases. For a finite system we have to calculate the surface area, $(A(x,y))$, for a given $x = n_1/N$ and $y = V_1/V$, The surface contribution of the free energy can be obtained from

$$F_{\text{surf}}(x,y) = \gamma A(x,y)\,, \tag{56}$$

where γ is the interfacial tension. In order to calculate $A(x,y)$ we assume that the surface area will have its minimum value for each x and y. If we

perform a simulation with the normal periodic boundary conditions, we can assume that the surface energy is minimized either by a drop of liquid, a drop of gas, or a double layer (see Fig. 7). The volumes of the droplets or double layer can be expressed easily in terms of x and y (see Ref. [9] for details). In Fig. 8 we plotted the function $A(x,y)/V^{2/3}$ on the x,y plane. This plot shows that there are two minima, which correspond to the case where there is only vapour or liquid in the subsystems (no interface, so $A(x,y) = 0$). Furthermore, it shows that there are large parts of the x,y plane where the gradient towards these minima is very small. It is possible that a simulation becomes trapped in such a region. An example of such a simulation is described in section 5.

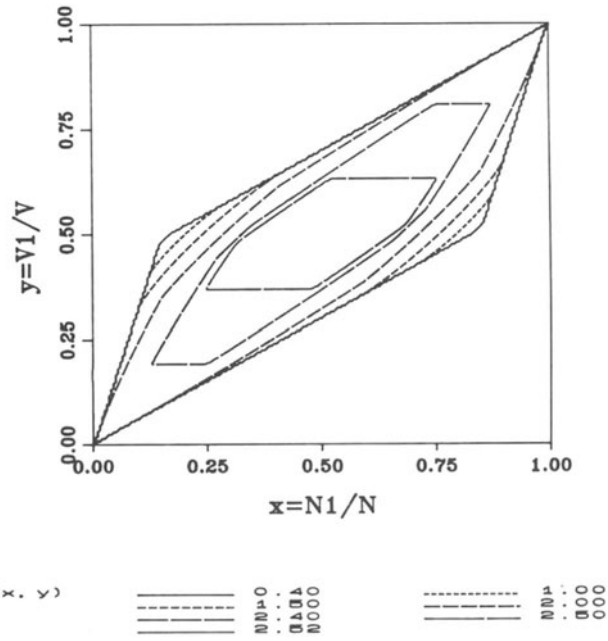

Fig. 8. A contour plot in the x,y plane ($x = n_1/N, y = V_1/V$) of the surface contribution ($a(x,y)$) to the free energy of the Gibbs ensemble. Note that the x,y values of the coexisting vapour and liquid phase are chosen arbitrarily.

It is interesting to calculate the probability of finding the density ρ in one of the sub-volumes for a finite system. This should be given approximately by

$$P(\rho) = \frac{\iint_S \mathrm{d}x\mathrm{d}y\, \delta(\frac{x}{y} - \rho) \exp\left[-\beta F_{\mathrm{surf}}(x,y)\right]}{\iint_S \mathrm{d}x\mathrm{d}y\, \exp\left[-\beta F_{\mathrm{surf}}(x,y)\right]}. \tag{57}$$

In order to study the temperature dependence, we have assumed that, close

to the critical temperature, the interfacial tension depends on the temperature according to [25]

$$\gamma = \gamma_0 (1 - T/T_c)^{\mu}, \tag{58}$$

where μ is the critical exponent for the interfacial tension (for three dimensional systems $\mu = 1.26$ [25]). The area S is defined by the densities of the coexisting gas and liquid phases at the given temperature (cf. eqn (27)).

When the system is infinite, we have (combining eqns (36), (33), and (57))

$$P(\rho) = \frac{1}{2}\delta(\rho - \rho_g) + \frac{1}{2}\delta(\rho_l - \rho). \tag{59}$$

However, for a finite system, function (57) exhibits interesting behaviour.

In Figs. 9 (a) and (b) we have plotted $P(\rho)$ for a Lennard-Jones fluid ($\gamma_0 = 2.71$ [25] and $T_c = 1.32$ [8]) for 64 and 216 particles respectively. These figures demonstrate that, as the temperature is increased, the following transitions can be observed. Since at low temperature the surface tension is large, it is unlikely that vapour and liquid will coexist in the same sub-volume. Therefore, at low temperature there are two sharp peaks, which correspond to the two coexisting phases. As the temperature increases, the surface tension decreases and becomes comparable to the entropy associated with the formation of an interface (there are simply more overall densities where vapour and liquid can coexist). Note that around $x = y$ the interface will be a double layer, and therefore small deviations around this line do not change the surface free energy contribution (see Figs. 7 and 8). Furthermore, $x = y$ is the longest 'strip' in the x, y plane on the surface S. These entropic considerations predict the appearance of a third peak at the average density ρ. When the temperature is increased further this entropy effect will dominate the surface contribution and the peaks of the coexisting phases will disappear close to, but below, the critical temperature of the finite system.

Note that the temperature range over which these transitions occur depends on the number of particles. Comparison with the results for 64 particles (Fig. 9 (a)) shows that the third peak exists over a larger temperature range.

It is interesting to compare these results with probability distributions for the densities obtained from simulations for the Lennard-Jones fluid. In Fig. 10 the results are presented for simulations with 216 particles at $T = 1.30$ (a) and $T = 1.31$. Comparison with the theoretical results (Fig. 9 (b)) shows not only that the transitions from two peaks at low temperatures to three peaks and finally to one peak below the critical temperature are observed but also that the temperature range of these transitions is in good agreement with the theoretical predictions.

(a) $N = 64$

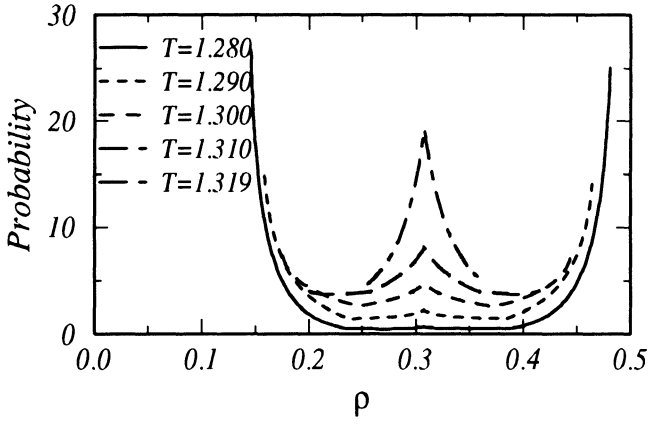

(b) $N = 216$

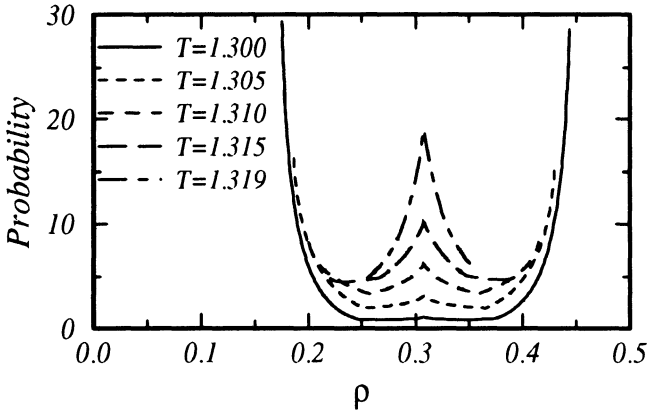

Fig. 9. The calculated density probability functions for a Lennard-Jones fluid (eqn (57)) at different temperatures for (a) $N = 64$ particles and (b) $N = 216$ particles. Note that in each figure the temperatures are different and that the curves are drawn for $\rho_g(T) < \rho < \rho_l(T)$.

(a) $T = 1.30$

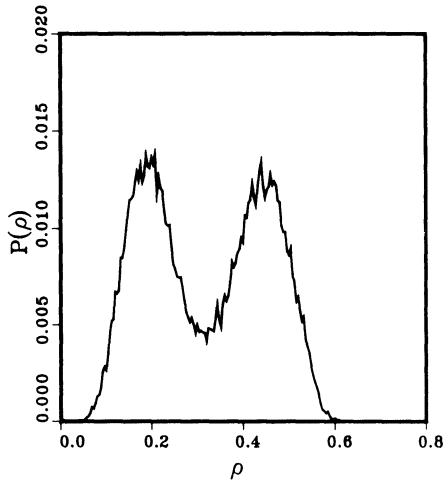

(b) $T = 1.31$

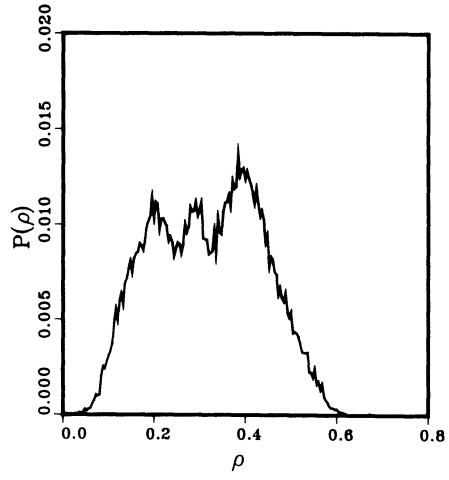

Fig. 10. The density probability functions for a Lennard-Jones fluid as obtained from simulations ($N = 216$) at two temperatures. These probability functions were obtained by calculating each cycle the volumes of the subsystems and densities in both subsystems and updating a histogram. At the end of the simulations these histograms were divided by the total number of cycles.

This theoretical analysis suggests that, in the Gibbs ensemble, finite-size effects can be expected which result in an underestimation of the critical temperature of the *finite* system. So, in the Gibbs ensemble, we are faced with finite-size effects of the opposite sign which will partly cancel. Therefore we can expect that the finite-size effects are smaller in this ensemble compared with conventional simulations. This would lead to a better estimate of the critical temperature of the infinite system. It would be interesting to see whether the arguments given above can be put on a more rigorous footing using finite-size scaling techniques.

In the above discussion it is assumed that eqn (58) is valid for a finite system. This assumption breaks down close to the critical temperature where we have to take into account finite-size rounding [26]. If we take these effects into account the interfacial tension is given by

$$\gamma \propto \gamma_0 (1 - T/T_c)^{2\nu} \tilde{f}(L/\xi)\,, \tag{60}$$

where $\tilde{f}(L/\xi)$ is a scaling function and ξ is the correlation length. For temperatures where $L \gg \xi$, eqn (60) reduces to eqn (58). However, close to T_c, if $L \ll \xi$ eqn (60) becomes

$$\gamma \propto \gamma_0 \frac{1}{\xi^2} \times \frac{\xi^2}{L^2} = \gamma_0 \frac{1}{L^2}\,. \tag{61}$$

As a result, the interfacial contribution to the free energy does not go to zero but to a constant value. If one takes this into account in the calculation of the density probability function, compare eqn (57), a third peak will only occur if γ_0 is sufficiently small. At present not much is known about the numerical value of γ_0, which will depend on the details of the intermolecular potential. Therefore it remains to be seen whether a third peak can be observed in a given system.

The finite-size effects for the simulations of phase coexistence in the Gibbs ensemble have been studied in detail by Mon and Binder [26]. In contrast to the theoretical arguments presented here, which predict that the Gibbs ensemble suffers less from finite-size effects than other ensembles, Mon and Binder conclude that the numerical magnitude of finite-size effects in the Gibbs ensemble and in the grand-canonical ensemble are very similar. In fact, detailed inspection of the results presented in Ref. [26] shows that the finite-size effects in the Gibbs ensemble are slightly larger. An important point is that Mon and Binder considered a two dimensional lattice gas. Furthermore, a "restricted" version of the Gibbs ensemble technique was used in which the volume fluctuations are suppressed. For this version of the Gibbs ensemble, we can also estimate the shape of the $P(\rho)$ curve using the same arguments as described above. The difference is that we now have to consider only the parameter x (no volume fluctuations, so y is constant).

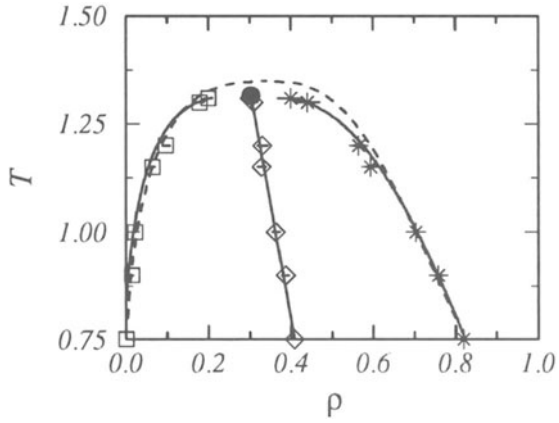

Fig. 11. The phase diagram of the Lennard-Jones fluid (with tail corrections, see [27] for details). The solid lines are the fits to the scaling law and the rectilinear law. The dashed line is the e.o.s. of Nicolas [3]. The points are the simulation results of [8, 9, 28], • is the estimate of the critical point. The simulation are performed with 108, 256, and 512 particles and show no systematic deviations.

As a result, the entropic contributions, which give rise to the third peak and result in an underestimation of the critical point, are completely suppressed. As a result, the theoretical arguments described here for the restricted form of the Gibbs ensemble would predict that the finite-size effects would be comparable to those in other ensembles.

An interesting point that follows from the work of Mon and Binder is the striking difference of the magnitude of the finite-size effects in lattices and continuum systems. For example, the results of Mon and Binder for the two-dimensional lattice gas show that a system of 100 spins overestimates the critical temperature of the infinite system by 20%. While in the results of Gibbs ensemble simulations of the two-dimensional Lennard-Jones fluid could not be detected [29] (see Fig. 11). More careful studies of the finite-size effects in continuum systems have been reported by Rovere *et al.* [30] and Wilding and Bruce [31]. finite-size scaling techniques, as developed for lattice models [24], are applied to the two-dimensional Lennard-Jones fluid. In lattice models the critical density is usually known from symmetry arguments and the critical point is can always be located by changing the temperature. In a continuum system the critical density has to be determined for each system size very accurately before one can apply the scaling techniques. Furthermore, these studies have been performed using many different cut-off values of the Lennard-Jones potential which has a significant influence on

the phase diagram [29, 32]. As a result, the importance of finite-size effects in the simulation of a continuum model is still unclear. These studies do show, however, that in contrast to lattice simulations, finite-size effects in continuum systems are significantly smaller and harder to detect.

5. Analyzing the results

Assuming that we have a working algorithm for performing a Monte Carlo simulation in the Gibbs ensemble, we should address the question as to whether the numbers that are generated in a simulation are reliable. First of all, the equilibrium conditions should be fulfilled:

- the pressure in both subsystems must be equal;
- the chemical potential must be equal in both phases.

Unfortunately, the chemical potential and the pressure of the liquid phase are subject to relatively large fluctuations, and therefore the observation that the equilibrium conditions have been fulfilled (within the statistical error) is not always sufficient. In this section we introduce some methods to analyze the data and to judge whether a simulation has been successful.

5.1. IS THE SIMULATION RELIABLE?

An example of a simulation for which the chemical potential and the pressure did not show significant deviations is shown in Fig. 12. In this figure an (x, y) plot of the simulation is given. In section 2.2 it was shown that in the thermodynamic limit the two points in the (x, y) plane which correspond to the coexisting liquid and gas density are sampled. In Fig. 12 we see that, in this simulation, a drift away from these two points has occurred. The reason that these drifts can occur becomes clear if we consider Fig. 8. This figure shows a contour plot of the surface contributions to the free energy of each (x, y) point. Besides the two global minima, which correspond to the densities of the coexisting gas and liquid phase, this figure shows that there are large areas in this plane where the gradient towards the global minima is small. Comparison with Fig. 12 shows that the simulation accidentally became trapped in such an area.

These fluctuations are not immediately apparent when the density probability function is considered, but the average gas and liquid densities can be influenced substantially. Therefore it is important to check for the consistency of the results by making a probability plot in the (x, y) plane.

Another simple indication of a drift in the (x, y) plane can be obtained from a probability distribution of the volumes. At a given temperature the densities of the coexisting phases are determined (but unknown) and because the total number of particles and total volume remain fixed, the probability function of the volume must have two (sharp) peaks if the simulation samples

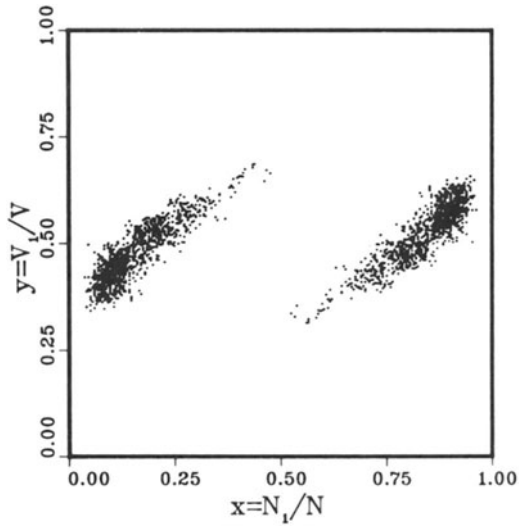

Fig. 12. The probability plot in the (x, y) plane for a Lennard-Jones fluid below the critical temperature ($T = 1.20$ and $N = 216$).

the (x, y) plane correctly. If this probability function does not give two sharp peaks, it is likely that the simulation is trapped in some metastable region.

Generally, if a simulation in the Gibbs ensemble is performed far below the critical temperature, it is not difficult to analyze the results. After the equilibration it becomes clear which of the boxes contains the vapour phase and which the liquid phase. The densities of the coexisting phases can simply be obtained by sampling the densities at regular intervals. For the estimation of the accuracy of the simulation one should be careful since these 'measured' densities are not sampled independently and in estimating the standard deviations of the results one should take this into account (this aspect is discussed in more detail in Appendix A of Ref. [33])

Close to the critical point, however, it is possible that the boxes continuously change 'identity' during a simulation. If, for such a system, the average density is calculated by calculating the average density in the two boxes, one would obtain the overall density. A more convenient method is to make a probability plot for an observed density in one of the boxes. In section 2.2 it was demonstrated that the two maxima of this curve correspond to coexisting vapour and liquid densities. Because this curve is obtained by sampling the density in both boxes, the results are not influenced when the boxes change identity. From this curve, an estimate of the densities can be obtained even very close to the critical temperature (see for example

Fig. 10). Furthermore, it is also clear from section 4 that the appearance of a third peak between the vapour and the liquid peak is an indication that the temperature is very close to the critical temperature (see for example Fig. 10(b)).

5.2. DETERMINING THE CRITICAL POINT

In section 4 it was shown that, due to finite-size effects which are specific to the Gibbs ensemble, the coexistence of vapour and liquid cannot be observed *just below* the critical temperature. Therefore, the highest temperature at which the coexistence can be observed is not a proper estimate of the critical temperature of the system. In order to estimate the critical temperature the results can be fitted to the law of rectilinear diameters [34]

$$\frac{\rho_l + \rho_g}{2} = \rho_c + A\,|T - T_c|\,, \tag{62}$$

where $\rho_l(\rho_g)$ is the density of the liquid (gas) phase, ρ_c the critical density and T_c the critical temperature. Furthermore, the results are also fitted to the scaling law for the density[25]

$$\rho_l - \rho_g = B\,|T - T_c|^{\beta} \tag{63}$$

where β is the critical exponent (for three dimensional systems $\beta = 0.32$ and for two dimensional systems $\beta = 0.125$ [25]). A and B depend on the system and are obtained from the fit. Note that this scaling law is strictly valid only close to the critical temperature and should be corrected at lower temperatures. In most practical applications the results of the Gibbs ensemble are not sufficiently accurate to justify these higher order terms.

Vega *et al.* [35] used Gibbs ensemble data to determine the effective exponent β (the exponent is not fixed *a priori* but is a result of the fit). Vega *et al.* observed that, within the limited accuracy, the data could be described with an effective exponent β very close to the critical value of 0.32.

6. Applications

The Gibbs ensemble has been used to study the phase behaviour of a various systems. The results of these simulations are reviewed in Ref. [12]. Here we discuss those applications of the Gibbs ensemble for which the algorithm that has been used differs significantly from the one described in section 3.

6.1. DENSE LIQUIDS

At high densities the number of exchange steps can become very large and requires a significant amount of CPU time. This problem occurs also in

conventional grand canonical Monte Carlo simulations. Various methods, which are used to extend simulations in the grand canonical ensemble to higher densities, can also be used in the Gibbs ensemble. An example of such a technique is the so-called excluded volume map sampling. This technique, is based on the ideas of Deitrick *et al.* [36] and Mezei [37], and adopted by Stapleton and Panagiotopoulos [38] for the Gibbs ensemble. Before the energy of the particle which has to be inserted is calculated, a map of the receiving subsystem is made, by dividing this subsystem into small boxes which can contain at most one particle. These boxes are labelled when they contain a particle. This map can then be used as a look-up table to check whether there is 'space' for the particle to be inserted. If such space is not available the trial configuration can be rejected immediately.

6.2. POLAR AND IONIC FLUIDS

Because of the long range of the dipolar and Coulombic interactions, the dipolar and Coulombic potential can not simply be truncated. Special techniques, such as the Ewald summation or reaction field [39], have been developed to take into account the long-range nature of the potential in a simulation. It is a general (mis)belief that special techniques are only needed for quantities like the dielectric constant. For thermodynamic quantities it is commonly held that the differences between, for example, the Ewald summation and the minimum-image boundary conditions, are very small. It turns out that the phase diagram is very sensitive to the details of the way the long-range part of the potential is taken into account.

A study of the phase behaviour of the Stockmayer fluid (a Lennard-Jones potential plus a point dipole) [23, 40] using the Gibbs ensemble technique has shown that, without the Ewald summation, the N-dependence is much larger [41]. In fact, performing simulations in which the potential is simply truncated at half the box size can lead to wrong results. When the potential is long ranged, and simply truncated at half the box size, the effective potential is quite different for a large volume compared to a small volume. Since in the Gibbs ensemble the volume of a subsystem varies significantly, a situation can occur in which one volume is much larger than the other. The system then tries to find equilibrium between two boxes with *different* potentials.

Moreover, Panagiotopoulos [42] and Valleau [43, 44] have performed simulations of the restrictive primitive model (a hard-core potential with a point charge) to model an ionic solution. Panagiotopoulos used the Gibbs ensemble technique with Ewald summation, while Valleau used the density scaling technique [44] with the minimum image boundary condition. The results of the two studies turned out to be different. This suggests that the phase diagram is sensitive to the way the long-range interactions are taken

into account. Also for the simple Lennard-Jones fluid it is observed that the phase diagram is very sensitive to the details of the truncation of the potential [27, 29] and that these differences are by no means small.

6.3. HARD-CORE POTENTIALS

Most of the rules of thumb as described in section 3.2 are not valid for systems in which particles interact with a hard-core potential. A configuration can immediately be rejected once *one* overlap between hard cores has been detected. In general, rejecting a configuration takes much less computer time than accepting of a configuration. For the hard-core fluids one can utilize some of the techniques developed by Wood [45] for constant pressure simulations of hard disks and which have been extended by Frenkel [46] for simulations of non-spherical convex bodies, to reduce the computer costs significantly. Below, some of these techniques as used by Smit and Frenkel for Gibbs-ensemble simulations of the hard-core Yukawa fluid [47] are described.

A particle displacement. During the simulations a neighbour list for each particle can be made without adding much additional computer time. This list contains all particles within a radius equal to the maximum displacement. This list can be used to test for possible overlaps before the energy of the new configuration is calculated. As a result the computer time required for a rejected move is much less than the time required for an accepted move. Therefore, the optimum maximum displacement results in an acceptance ratio which is far less than the normal 50%.

A volume change. It is straightforward to keep track of the minimum distance between a pair of particles in each box during the simulations. After a volume change, the attempt can be rejected immediately if one of these minima becomes smaller than the hard-core radius.

A particle exchange. Before the energy is calculated one can check whether the particle that is inserted overlaps with one of the other particles.

6.4. MIXTURES

The Gibbs ensemble technique can also be extended to study the behaviour of mixtures. The appropriate acceptance rules are given in Ref. [15]. Examples of mixtures that have been studied using the Gibbs ensemble technique are mixtures of Lennard-Jones particles [15, 48, 49].

One of the main problems in studying liquid-liquid systems is that both phases are relatively dense. It is therefore difficult to exchange particles between the two phases, in particular when the components differ significantly in size. For phase equilibria in mixtures it is sufficient that the chemical potential of one of the components, labelled i, is equal in both phases and for

the other components only the difference between the chemical potential and the chemical potential of component i needs to be equal in the two phases. For a simulation this observation implies that it is sufficient to specify the chemical potential of one of the components and the differences for the others. Such simulations are called semi-grand canonical ensemble simulations [50]. In a simulation one can ensure that the difference in chemical potential between two components is constant by performing Monte Carlo moves in which the identity of the particles is changed.

The ideas of the semi-grand canonical ensemble simulations have been adopted by Panagiotopoulos [51] for the Gibbs ensemble. Instead of attempts to insert and remove particles for both components, only the smallest particles are inserted, while for the larger particles only moves involving a change of identity are used.

When mixtures are studied which are symmetric with respect to particle interchange, the density or compositions of the two phases must be equal by symmetry. As a result it is not necessary to perform volume changes [52, 53].

6.5. CHAIN MOLECULES

The applications of the Gibbs ensemble as described above are all limited to model systems containing atoms or small molecules. Using the conventional (random) sampling schemes, successful insertions can only be achieved for small molecules. At typical liquid densities, the probability of a successful insertion of a monomer is of the order of 0.5%; the probability of inserting a chain of eight of these monomers is less than 10^{-18}. Such a low probability of insertion would necessitate a prohibitive amount of computer time. Here we show that configurational-bias Monte Carlo techniques (see Frenkel's contribution, Chapter 4 in this volume) can be combined with the Gibbs ensemble method [54, 55].

We can use the configurational-bias scheme [56] to grow the chains in such a way that the "holes" in the system are found. However, such a scheme of insertion would bias the simulations if the ordinary acceptance rules were used. The correct distribution of configurations can be sampled if the acceptance rule for this step is modified.

Consider a trial move to remove a molecule from one box (say, 1) and insert it in the other box (2). To achieve this, we insert a chain molecule in box 2, using a stepwise method. First, we attempt to insert a single monomer in box 2. Next, k random trial segments are generated, such that the next monomeric unit is located somewhere on a spherical shell around the first monomer. For each of these trial segments, the potential energy due to interaction with the other particles in the system is calculated, and one

of the directions, say direction i, is selected with a probability given by

$$P_2(n) = \frac{\exp[-\beta v_2(i)]}{\sum_{j=1}^{k} \exp[-\beta v_2(j)]}, \tag{64}$$

where $\beta = 1/k_B T$ and $v(j)$ is the energy of a j-th trial direction and n labels the position of the segment in the chain. The subscript (in this case, 2) indicates the box in which these quantities are calculated. In addition, we compute a weight factor

$$W_2(n) = \left(\sum_{j=1}^{k} \exp[-\beta v_2(j)] \right) W_2(n-1). \tag{65}$$

Note that $W_2(0)$, the weight factor for the monomer, is simply the Boltzmann factor associated with the random insertion of a monomer. At the same time we calculate a corresponding weight factor $W_1(n)$ for the chain that we chose to remove from box 1

$$W_1(n) = \left(\sum_{j=1}^{k} \exp[-\beta v_1(j)] \right) W_1(n-1), \tag{66}$$

where the summation is over the same set of trial directions as in box 2, with the restriction that the orientation that is selected in box 2 is replaced by the actual orientation of the chain in box 1 of that particular segment. This procedure is repeated until the chain has the desired length ($n = l$).

To derive the appropriate acceptance rules, we impose detailed balance on our Monte Carlo procedure. This implies that, in equilibrium, the rate at which particles are moved from box 1 to 2 equals the reverse rate:

$$N(1)\, P(1|2)\, \mathrm{acc}(1|2) = N(2)\, P(2|1)\, \mathrm{acc}(2|1). \tag{67}$$

Note that we now have to take into account the probability that, starting from the current configuration, a configuration 2 is generated with $n_1 - 1$ particles in box 1 ($P(1|2)$) (compare section 3). The ratio of the statistical weights $N(1)$ and $N(2)$ follows from eqn (46). Substitution of this into eqn (67), using eqns (64)–(66) we find that the following acceptance rule for the exchange step will satisfy the detailed balance condition

$$\mathrm{acc}(1|2) = \min\left(1, \frac{n_1(V - V_1)}{(N - n_1 + 1)V_1} \frac{W_2}{W_1}\right). \tag{68}$$

This demonstrates that we can use the biased insertion and still sample the correct distribution of configurations, provided that we use the acceptance rules given by eqn (68). At this stage, it is worthwhile pointing out that, with trivial extensions, the above scheme can be applied to mixtures of chain molecules.

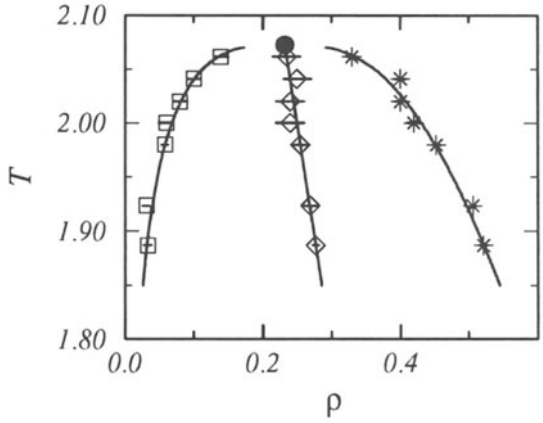

Fig. 13. Liquid-vapour coexistence curve of a system of 200 chains of 8 Lennard-Jones monomers. The monomers are connected by bonds of a fixed length σ. The bonds are allowed to rotate freely with respect to each other. The monomer-monomer interaction is modeled by a Lennard-Jones potential that is cut off at a radius $R_c = 2.5\sigma$ and shifted. The estimate of the critical point is indicated by a black dot. (Figure from Ref. [54])

An illustration of the scheme described above is shown in Fig. 13, This figure gives the phase diagram of a chain of eight Lennard-Jones 'monomers' [54]. This scheme has also been applied successfully to determine the phase diagram of alkanes by de Pablo *et al.* [55].

Acknowledgements

I would like to thank Daan Frenkel, Philip de Smedt, Kurt Binder, and Monica van Leeuwen for many useful discussions and suggestions.

References

[1] D. Frenkel, Free energy computations and first order phase transitions, in *Molecular Dynamics Simulations of Statistical Mechanics Systems*, edited by G. Ciccotti and W. G. Hoover, Proceedings of the 97th Int. Enrico Fermi School of Physics, 1986.

[2] J. M. Prausnitz, R. N. Lichtenthaler, and E. Gomes de Azevedo, *Molecular Thermodynamics of Fluid-Phase Equilibria*, Prentice-Hall, Englewood Cliffs N. J., second edition, 1986.

[3] J. J. Nicolas, K. E. Gubbins, W. B. Streett, and D. J. Tildesley, *Molec. Phys.* **37**, 1429 (1979).

[4] J. K. Johnson, J. A. Zollweg, and K. E. Gubbins, *Molec. Phys.* , in press.

[5] M. R. Reddy and S. F. O'Shea, *Can. J. Phys.* **64**, 677 (1986).

[6] B. WIDOM, *J. Chem. Phys.* **39**, 2802 (1963).

[7] K. S. SHING and K. E. GUBBINS, *Molec. Phys.* **45**, 129 (1982).

[8] A. Z. PANAGIOTOPOULOS, *Molec. Phys.* **61**, 813 (1987).

[9] B. SMIT, P. DE SMEDT, and D. FRENKEL, *Molec. Phys.* **68**, 931 (1989).

[10] D. FRENKEL, Monte Carlo simulations, in *Computer Modelling of Fluids, Polymers and Solids*, edited by C. R. A. CATLOW, S. C. PARKER, and M. P. ALLEN, Kluwer Academic Publishers, 1990.

[11] B. SMIT and D. FRENKEL, *Molec. Phys.* **68**, 951 (1989).

[12] A. Z. PANAGIOTOPOULOS, *Molec. Simul.* **9**, 1 (1992).

[13] D. RUELLE, *Statistical Mechanics: Rigorous Results*, Benjamin, Reading Massachusetts, 1969.

[14] R. B. DINGLE, *Asymptotic Expansions, their Derivation and Interpretation*, Academic Press, 1973.

[15] A. Z. PANAGIOTOPOULOS, N. QUIRKE, M. STAPLETON, and D. J. TILDESLEY, *Molec. Phys.* **63**, 527 (1988).

[16] P. SINDZINGRE, G. CICCOTTI, C. MASSOBRIO, and D. FRENKEL, *Chem. Phys. Lett.* **136**, 35 (1987).

[17] K. SHING and S. T. CHUNG, *J. Phys. Chem.* **91**, 1674 (1987).

[18] N. G. VAN KAMPEN, *Stochastic Processes in Physics and Chemistry*, North-Holland, Amsterdam, 1981.

[19] W. FELLER, *An Introduction to Probability Theory and its Applications*, volume 1, Wiley, New York, 1957.

[20] W. FELLER, *An Introduction to Probability Theory and its Applications*, volume 2, Wiley, New York, 1966.

[21] P. EPPENGA and D. FRENKEL, *Molec. Phys.* **52**, 1303 (1984).

[22] I. R. MCDONALD, *Molec. Phys.* **23**, 41 (1972).

[23] B. SMIT, C. P. WILLIAMS, E. M. HENDRIKS, and S. W. DE LEEUW, *Molec. Phys.* **68**, 765 (1989).

[24] K. BINDER, *Z. Phys. B. Cond. Mat.* **43**, 119 (1981).

[25] J. S. ROWLINSON and B. WIDOM, *Molecular Theory of Capillarity*, Clarendon Press, Oxford, 1982.

[26] K. K. MON and K. BINDER, *J. Chem. Phys.* **96**, 6989 (1992).

[27] B. SMIT, *J. Chem. Phys.* **96**, 8639 (1992).

[28] B. SMIT and C. P. WILLIAMS, *J. Phys. Cond. Mat.* **2**, 4281 (1990).

[29] B. SMIT and D. FRENKEL, *J. Chem. Phys.* **94**, 5663 (1991).

[30] M. ROVERE, D. W. HERMANN, and K. BINDER, *J. Phys. Cond. Mat.* **2**, 7009 (1990).

[31] N. B. WILDING and A. D. BRUCE, *J. Phys. Cond. Mat.* **4**, 3087 (1992).

[32] J. E. FINN and P. A. MONSON, *Phys. Rev. A* **39**, 6402 (1989).

[33] B. SMIT, *Computer simulation of phase coexistence: from atoms to surfactants*, PhD thesis, Rijksuniversiteit Utrecht, The Netherlands, 1990.

[34] J. S. ROWLINSON and F. L. SWINTON, *Liquids and Liquid Mixtures*, Butterworth, London, third edition, 1982.

[35] L. VEGA, E. DE MIGUEL, L. F. RULL, G. JACKSON, and I. A. MCLURE, *J. Chem. Phys.* **96**, 2296 (1992).

[36] G. L. DEITRICK, L. E. SCRIVEN, and H. T. DAVIS, *J. Chem. Phys.* **90**, 2370 (1989).

[37] M. MEZEI, *Molec. Phys.* **40**, 901 (1980).

[38] M. R. STAPLETON and A. Z. PANAGIOTOPOULOS, *J. Chem. Phys.* **92**, 1285 (1990).

[39] M. P. ALLEN and D. J. TILDESLEY, *Computer Simulation of Liquids*, Clarendon, Oxford, 1987.

[40] M. E. VAN LEEUWEN, B. SMIT, and E. M. HENDRIKS, *Molec. Phys.* (1992), in press.

[41] D. J. TILDESLEY, private communication, 1989.

[42] A. Z. PANAGIOTOPOULOS, *Fluid Phase Equilibria* **76**, 97 (1992).

[43] J. P. VALLEAU, *J. Chem. Phys.* **95**, 584 (1991).

[44] J. P. VALLEAU, *J. Comput. Phys.* **96**, 193 (1991).

[45] W. W. WOOD, *J. Chem. Phys.* **52**, 729 (1970).

[46] D. FRENKEL, (private communications), 1990.

[47] B. SMIT and D. FRENKEL, *Molec. Phys.* **74**, 35 (1991).

[48] M. E. VAN LEEUWEN, C. J. PETER, J. DE SWAAN ARONS, and A. Z. PANAGIOTOPOULOS, *Fluid phase equilibria* **66**, 57 (1991).

[49] V. I. HARISMIADIS, N. K. KOUTRAS, D. P. TASSIOS, and A. Z. PANAGIOTOPOULOS, *Fluid phase equilibria* **65**, 1 (1991).

[50] D. A. KOFKE and E. D. GLANDT, *Molec. Phys.* **64**, 1105 (1988).

[51] A. Z. PANAGIOTOPOULOS, *Int. J. Thermophys.* **10**, 447 (1989).

[52] J. G. AMAR, *Molec. Phys.* **4**, 739 (1989).

[53] R. D. MOUNTAIN and A. H. HARVEY, *J. Chem. Phys.* **94**, 2238 (1991).

[54] G. C. A. M. MOOIJ, D. FRENKEL, and B. SMIT, *J. Phys. Cond. Mat.* **4**, L255 (1992).

[55] M. LASO, J. J. DE PABLO, and U. W. SUTER, *J. Chem. Phys.* **97**, 2817 (1992).

[56] D. FRENKEL, G. A. M. MOOIJ, and B. SMIT, *J. Phys. Cond. Mat.* **4**, 3053 (1992).